

Modeling and measurement of a micro-optic beam deflector

Tom D. Milster

University of Arizona, Optical Sciences Center
Tucson, Arizona 85721

J. Nan Wong

Lawrence Livermore National Laboratory
Livermore, California 94550**ABSTRACT**

We investigate the use of a unity-magnification micro-optic beam deflector. The deflector consists of two arrays of positively powered lenslets. The lenslets on each array are arranged in a square grid. Design criteria are based on usefulness in optical data storage devices. The deflector is designed to operate over a $\pm 1.6^\circ$ range of deflection angles. We compare modeling results with interferometric analysis of the wavefront from a single lenslet pair. Our results indicate that the device is nearly diffraction limited, but there are substantial wavefront errors at the edges and corners of the lenslets.

1. INTRODUCTION

There are many ways to achieve fine position control in optical data storage systems. Most rely on the translational movement of an objective lens. Other methods rely on changing the angular position of the beam before the objective lens, as shown in Figure 1. Angular beam deflection for data storage has been discussed with respect to galvanometers^{1,2} and acousto-optic cells³. There are other possibilities, which include prisms, electro-optic cells and holograms, but they are not well suited for data storage due to either performance limitations, massive components, or complicated electronics. Galvanometer mirrors provide the necessary function and achieve good bandwidth, but they have two disadvantages. First, they disturb the beam path beyond what is required for deflection at the objective lens. This is not a performance limitation, but it is a practical one. The beam path in an optical data storage device must be as compact as possible. Any unnecessary deviations in the beam path result in extra real estate that must be used to satisfy design requirements. Secondly, reflections off of a mirrored surface require that the surface be of extremely high quality. The surface quality is difficult to achieve in a lightweight mirror, which is a requirement for high bandwidth. In addition, as the lightweight mirror is rotated, vibrational modes of the mirror surface can affect beam quality. These considerations can be overcome with good engineering, but additional costs associated with the components are likely. There are also disadvantages to using acousto-optic cells for beam deflection. The primary disadvantages are cost and complexity of the electronics. What we seek is a low-cost alternative to these techniques that does not disturb the beam path beyond what is necessary for fine positioning.

An alternative technique for beam steering is to use two lenses arranged as an afocal telescope, as shown in Figure 2A. As one of the lenses is translated, the output beam is

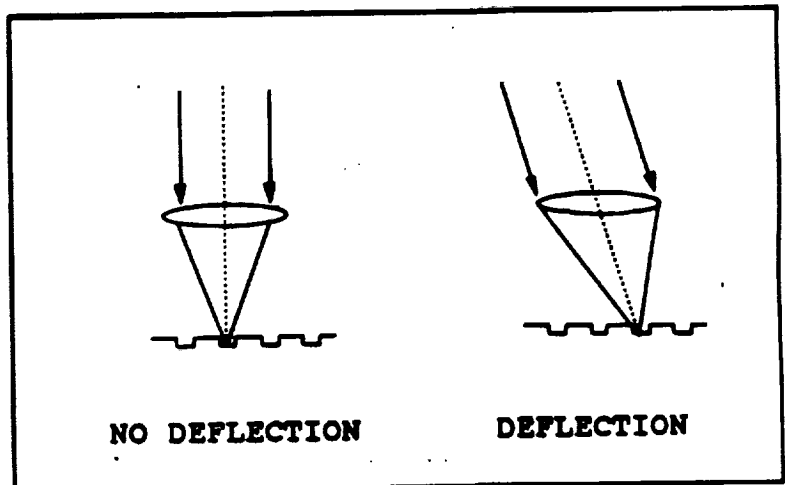


Figure 1. Angular deflection of the beam before the objective lens.

deflected. In order to avoid problems with aberrations, the lenses must operate at relatively high $f/\#$, which results in a large form factor. The lenses are massive and require significant power from an actuator to achieve high bandwidth. The range of deflection is another disadvantage of this system. Since the $f/\#$ of the objective lens is typically $f/1$ and the telescope must be $f/5$ or greater, the translation of beam steering lens must be at least five times the distance required at the disk plane. As described, the afocal relay deflector is not useful as a beam steering device for optical data storage.

Instead of using two large lenses, we suggest using two arrays of micro-optic lenses, as shown in Figure 2B. Each lenslet pair performs as the afocal telescope in Figure 2A. The focal lengths of the lenslets are much shorter than the two-lens system, so the device is much more compact. The mass of a lenslet array is significantly less than the mass of a single lens, so high bandwidth can be achieved. The translation of the micro-lens array is much smaller than that required in the two-lens system. A similar device was discussed by Goltsov and Holz⁴, as shown in Figure 3. Instead of two positively powered arrays, they use one positively powered array and one negatively powered array. As one array is translated relative to the other, the output beam is deflected. This device does not satisfy our requirement for unity magnification through the system. Also, the positive-negative system does not fill the output beam, which results in a complicated diffraction pattern at the disk plane. Conversely, the positive-positive system uniformly fills the output with unity magnification.

In the following paragraphs, we describe our device in detail. First, we describe system requirements for an optical data storage system. CODE V modeling is used to predict performance of the device. We then discuss boundary losses and the implementation of field lenses to limit these losses. Diffraction calculations are used to predict the pattern observed on the disk plane. Our experimental data include interferometric analysis of the lenslets. Finally, we draw conclusions from our work.

2. THEORY AND MODELING

Table I lists the operating requirements of the beam steering device. These numbers are based on typical values for the wavelength and aperture size used in optical data storage devices. The $\pm 1.6^\circ$ range of deflection angles corresponds to about $\pm 120 \mu\text{m}$ of fine positioning at the disk plane with an $f/1$ objective lens. If the track pitch is $1.6 \mu\text{m}$, ± 75 tracks can be accessed with the beam steering device. The field angle

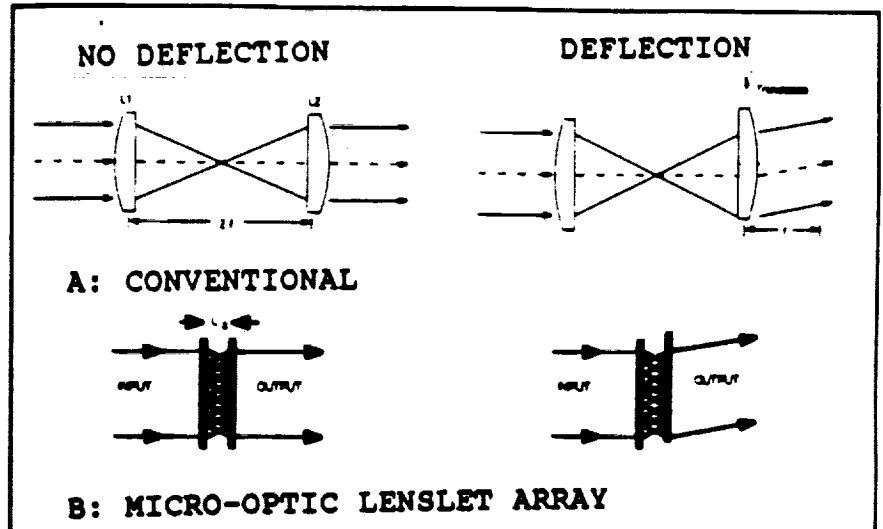


Figure 2. A: Conventional refractive beam deflector. B: Lenslet array beam deflector.

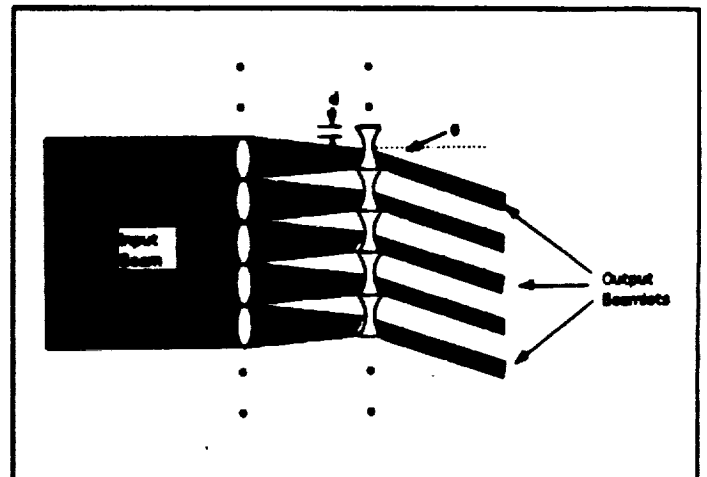


Figure 3. Schematic illustration of Goltsov and Holz device.

requirement of $\pm 0.5^\circ$ is to allow for some alignment tolerance.

We tested Monolithic Lenslet Modules¹ (MLMs), which are refractive microlens arrays in close-packed geometries. Our MLM arrays consisted of $400\mu\text{m}$ square lenslets on a grid spaced $400\mu\text{m}$ apart. Lenslets are formed in a thin layer of a single-part epoxy that has been molded on a substrate. In our case, the substrate material was a 1.27 mm thick piece of soda lime glass. The lenslets resemble simple plano-convex lenses. The advertised focal length for the arrays is 3.20 mm at $\lambda = 633\text{ nm}$. Our estimate of the focal length at $\lambda = 830\text{ nm}$ is 3.27 mm. The $f/\#$ is 5.8 if one uses the diagonal of the lenslet in the calculation. Since the arrays are refractive and not diffractive, we expect high transmission efficiency and relatively little sensitivity to small wavelength variations. The depth of focus, which is given by

$$\Delta z = \pm 2\lambda(f/\#)^2$$

calculates to $\pm 56\mu\text{m}$ at $\lambda = 830\text{ nm}$. The required translation for 1.6° is $91\mu\text{m}$.

CODE V was used to model the positive-positive array system. The lenslets were arranged as shown in Figure 2A, with the curved side toward the infinite conjugate. Wavefront profiles are shown in Figure 4 for the deflection system operating at $\lambda = 633\text{ nm}$. Figure 4A displays performance with no deflection. Figure 4B displays performance at 1.6° . In both cases, superb wavefronts of less than 0.05 waves peak to valley are predicted, which implies that diffraction-limited performance will be achieved.

The positive-positive system has one major loss mechanism. As the array is translated, the light that is incident on adjacent lenslets is lost, as shown in Figure 5. The boundary losses can be calculated by assuming square lenslets. The transmission efficiency of the system is given by

$$\eta = 1 - \sqrt{2} f/\# \tan \theta \quad (1)$$

where θ is the deflection angle. Therefore, we desire a low $f/\#$ in order to limit boundary losses.

Boundary losses can be virtually eliminated by using a field lens array, as shown in Figure 6. The field array is translated in unison with the last array. The field lenslets redirect the diverging beamlets so that they are centered and optimally fill the lenslets of the last array. The transmission efficiency of this system is given by

$$\eta' = 1 - f/\# \tan^2 \theta \quad (2)$$

A comparison of the transmission factors resulting from Equations 1 and 2 is given in Table II. For all field

Table I. System design parameters.

INPUT BEAM SIZE (DIAMETER)	4.3 mm
OUTPUT BEAM SIZE (DIAMETER)	4.3 mm
WAVELENGTH	$830 \pm 20\text{ nm}$
RANGE OF DEFLECTION ANGLES	$\pm 1.6^\circ$
FIELD ANGLE	$\pm 0.5^\circ$

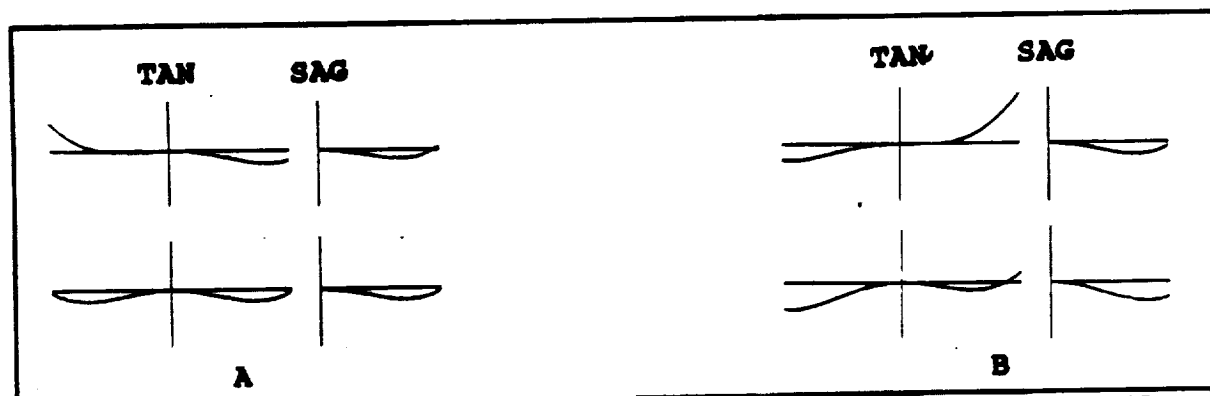


Figure 4. Wave fans resulting from a single lenslet. The maximum scale on the figures is ± 0.05 wave. Upper traces refer to performance at the maximum field angle. The arrays are set for: A) no deflection, and B) 1.6° deflection.

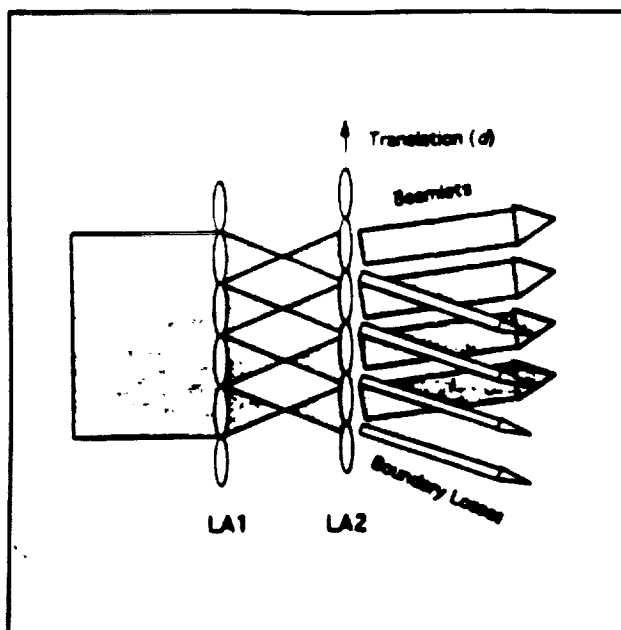


Figure 5. Boundary losses are due to the light incident on adjacent lenslets.

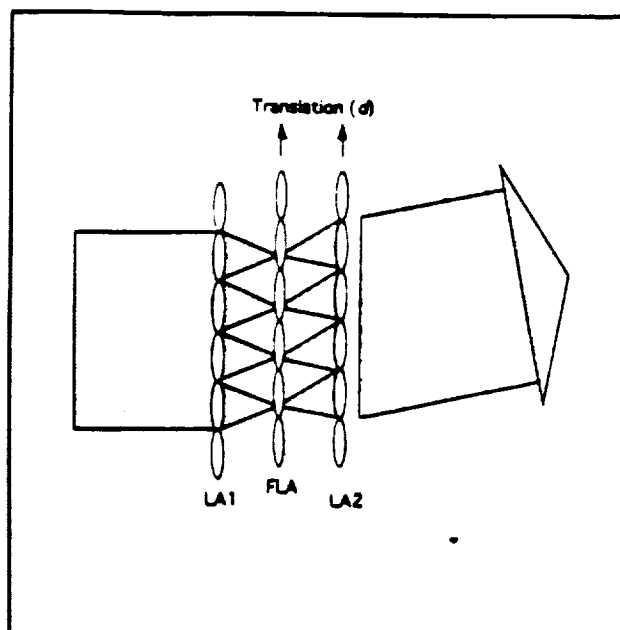


Figure 6. Losses due to boundary losses can be avoided by using a field-lens array. The field lens travels with LA2, the last array.

angles of interest, the addition of the field array significantly improves the transmission efficiency.

Another consideration for modeling is the diffraction pattern observed at the disk plane. The diffraction from each square lenslet results in a $(\sin \pi x)/\pi x$ distribution. Since the lenslets are spaced at a distance equal to their width, the zeros of the sinc function will coincide with higher orders of the diffraction pattern. Therefore, very little diffracted light should be observed. Figure 7 displays the result of a diffraction calculation for our system.

Table II. Efficiencies

Angle ($^\circ$)	η	η'
1.0	0.86	0.99
2.0	0.71	0.99
4.0	0.43	0.97

3. EXPERIMENT

A layout of the interferometric experiment is shown in Figure 8. Collimated light from a 780 nm laser diode passed through the MLMA. A unity-magnification afocal telescope was used to image LA2, the last lenslet array, into the 8X beam expander. A Laser Diode Interferometric Tester (LADITE) from WYKO corporation was used for the interferometric analysis. The LADITE is a phase shifting and self referencing interferometer. The image of the array from the beam expander was placed at the entrance pupil of the LADITE.

The fringe pattern observed in one of the measurements is shown in Figure 9. The boundary of the lenslets are clearly visible, and straight fringes are observed over a large percentage of the lenslets. The corner areas display a diamond-like pattern that does not give useful lens action. A dust spec is observed in the upper center lenslet. In general, very careful procedures were necessary in order to limit

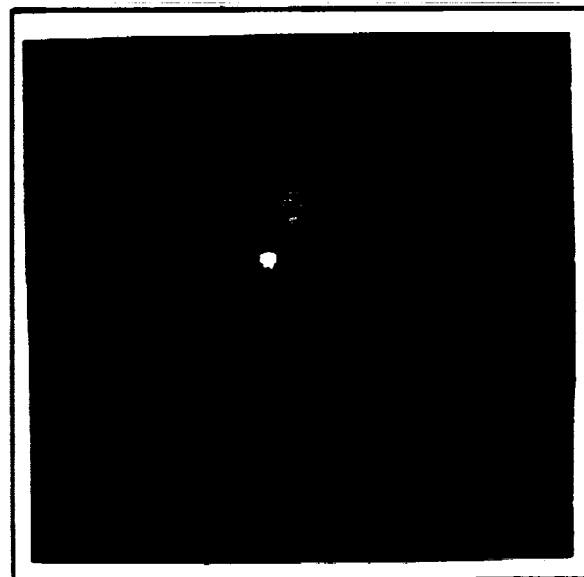


Figure 7. Far-field pattern predicted from a diffraction calculation of the lenslet arrays.

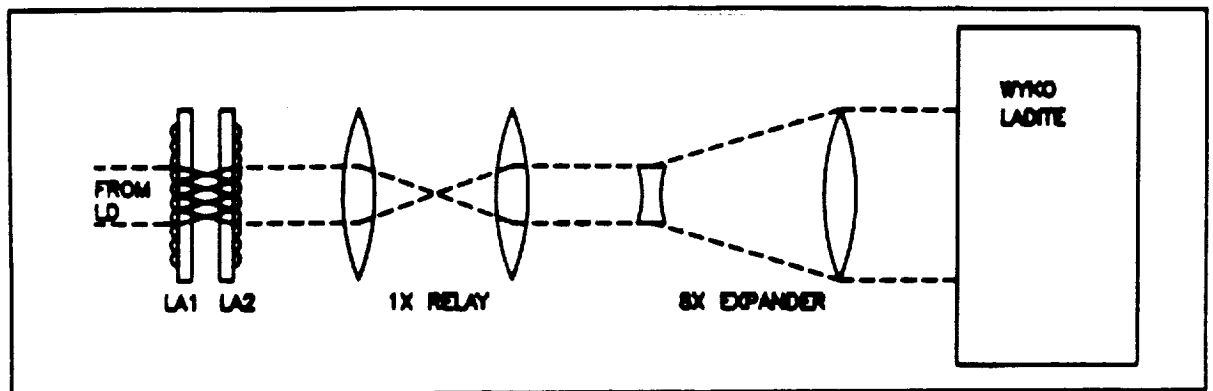


Figure 8 Experimental Layout.

contamination of the array. A small dust spec of $25\ \mu\text{m}$ to $50\ \mu\text{m}$ diameter could significantly affect the performance out of a lenslet. The epoxy material was also very easily scratched.

Before the MLM arrays were placed into the system, we obtained a reference map of the other optical components, which is subtracted from the data on the lenslets. When interferometric data were taken, one lenslets were masked individually. The best wavefront obtained for a lenslet was about 0.08 waves rms. Upon further investigation, we found that most of the wavefront error was located at the edge of the lenslets. Figure 10 displays an OPD map of the surface. The largest variations are observed in the corners and along the edges. Figure 11 displays an OPD profile of one edge of the lenslet. A large departure is observed near one corner of Figure 11. To illustrate this point further, Figure 12 displays the variation of wavefront quality observed on a typical lenslet when the mask size is reduced from the full aperture. Both a square and a round mask were used. It is clear that diffraction-limited performance can easily be achieved if performance in the corners and along the edges can be improved. We observed no significant change in wavefront characteristics as one array was translated up to $50\ \mu\text{m}$ relative to the other.

Figure 13 displays the beam deflector illuminated over the full 4.3 mm. We are in the process of evaluating the far-field pattern from this device.



Figure 9. Fringe observed through the LADITE.

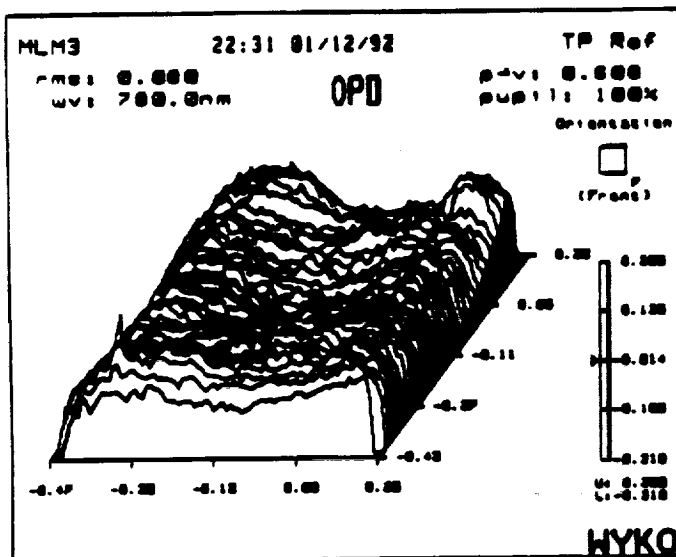


Figure 10. OPD map of one lenslet.

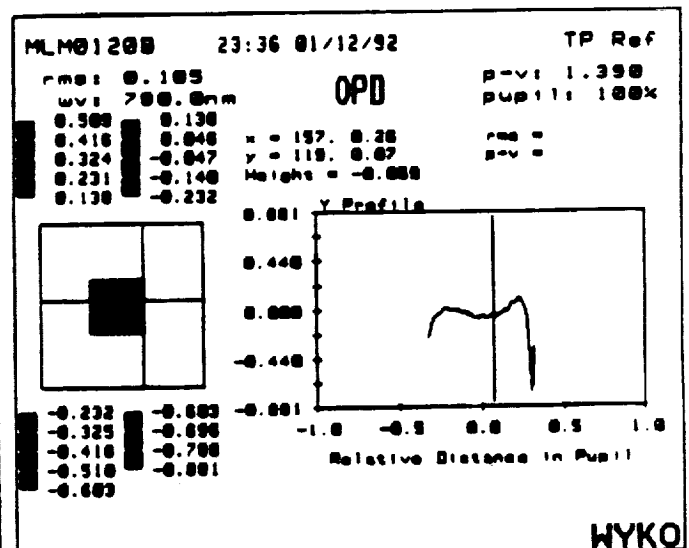


Figure 11. Edge OPD profile from a lenslet. The peak-to-peak variation at the edge is about 1.4 waves.

4. CONCLUSIONS

We have analyzed a beam deflector that consists of two arrays of refractive micro lenses. One array is translated in order to achieve deflection. Design analysis indicates that diffraction-limited performance is obtainable over a $\pm 1.6^\circ$ range of deflection angles. Boundary losses can be eliminated with the use of a micro-optic field lens array. Diffraction analysis indicates that a bright central spot should be observed in the far-field pattern. Measurement of the wavefront quality from individual lenslets indicates that the lenslets are of good wavefront quality. However, the edges and corners of the lenslets have significant aberration. We are in the process of evaluating the far-field pattern from a 4.3 mm diameter beam passing through the beam deflector.

5. ACKNOWLEDGEMENTS

The authors wish to thank Kevin Erwin and Mark S. Wang, both of the Optical Sciences Center at the University of Arizona, for their help in acquiring data for this report. We give our sincere thanks to Steve Martinick at WYKO Corporation for loaning us the LADITE. This work was partially sponsored by a grant from the Joint Services Optical Program, contract #F49620-91-C-0009. Additional support was provided by the Optical Data Storage Center, and student support was provided for J.N. Wong from Lawrence Livermore National Laboratory.

6. REFERENCES

1. D.K. Towner, "Scanning techniques for optical data storage," *SPIE Proceedings: Optical Mass Data Storage II*, vol. 695, pp. 172-180, 1986.
2. A. Takahashi, H. Ohsawa, N. Seo, T. Takahara, H. Yamazaki, and W. Shinohara, "High speed accessing of 90 mm optical disk drive," *SPIE Proceedings: Optical Data Storage*, vol. 1316, 1990.
3. K. Matsumoto and T. Maeda, "Acousto-optic accessing in optical disks," *Jap. J. Appl. Phys.*, vol. 28, supplement 28-3, pp. 335-340, 1989.
4. W. Goltsov and M. Holz, "Agile beam steering using binary optics microlens array," *Optical Engineering*, vol. 29, no. 11, pp 1392-1397, 1990.
5. Adaptive Optics Associates, commercial literature.

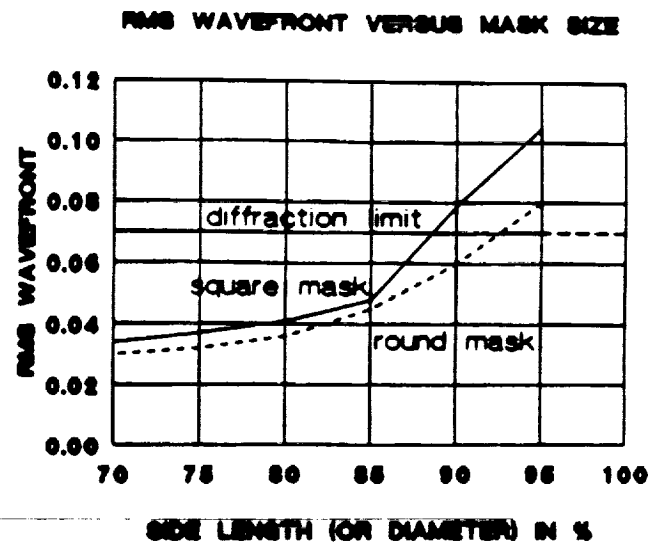


Figure 12. Wavefront variation as a function of mask diameter centered on the lenslet. The horizontal axis corresponds to the length of the mask: A) across one side of the square mask, B) across the diameter of the circular mask.

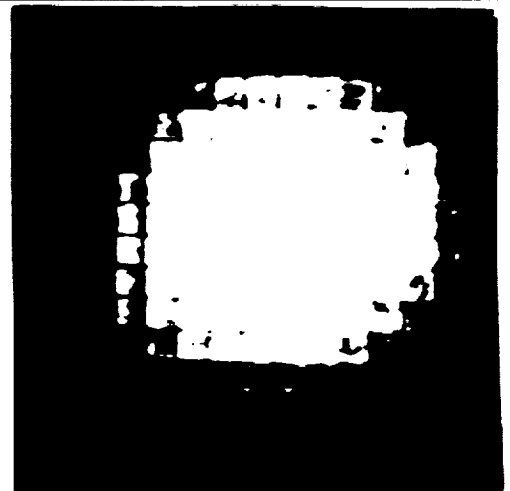


Figure 13. Beam deflector illuminated with a 4.3 mm laser beam.

APPENDIX J
